Title

Intramolecular Conformational Changes Optimize Protein Kinase C Signaling

Journal

Cell Chemical Biology, 21(4)

ISSN

2451-9456

Authors

Antal, Corina E

Violin, Jonathan D

Kunkel, Maya T

et al.

Publication Date

2014-04-01

DOI

10.1016/j.chembiol.2014.02.008

Peer reviewed

Published in final edited form as:
Chem Biol. 2014 April 24; 21(4): 459–469. doi:10.1016/j.chembiol.2014.02.008.

Intramolecular Conformational Changes Optimize Protein Kinase C Signaling[#]

Corina E. Antal[1,2], **Jonathan D. Violin**[3], **Maya T. Kunkel**[1], **Søs Skovsø**[1,4,5], and **Alexandra C. Newton**[1]

Alexandra C. Newton: anewton@ucsd.edu

[1]Department of Pharmacology, University of California at San Diego, La Jolla, CA, 92093, USA

[2]Biomedical Sciences Graduate Program, University of California at San Diego, La Jolla, CA, 92093, USA

[4]Institute for Cellular and Molecular Medicine, Panum Institute, University of Copenhagen, Blegdamsvej 3, DK-2200 Copenhagen, Denmark

Summary

Optimal tuning of enzyme signaling is critical for cellular homeostasis. We use fluorescence resonance energy transfer reporters in live cells to follow conformational transitions that tune the affinity of a multi-domain signal transducer, protein kinase C, for optimal response to second messengers. This enzyme comprises two diacylglycerol sensors, the C1A and C1B domains, whose intrinsic affinity for ligand is sufficiently high that the enzyme would be in a ligand-engaged, active state if not for mechanisms that mask its domains. We show that both diacylglycerol sensors are exposed in newly-synthesized protein kinase C and that conformational transitions following priming phosphorylations mask the domains such that the lower affinity sensor, the C1B domain, is the primary diacylglycerol binder. Protein kinase C's conformational rearrangements serve as a paradigm for how multi-module transducers optimize their dynamic range of signaling.

Keywords

optimized signaling; conformational transitions; fluorescence resonance energy transfer; protein kinase C; C1 domain

[#]Running title: Live Cell Imaging of PKC's Conformational Changes

Correspondence to: Alexandra C. Newton, anewton@ucsd.edu.

[3]Present address: Trevena Inc., King of Prussia, PA, 19406, USA

[5]Present address: In Vivo Pharmacology Graduate Program, Faculty of Health and Medical Sciences, University of Copenhagen, Blegdamsvej 3, DK-2200 Copenhagen, Denmark

Introduction

The use of modules to build recognition in signal transducing proteins is at the crux of signaling networks (Pawson, 1995, 2007). The serine/threonine kinase, protein kinase C (PKC), epitomizes the use of multiple modules to effectively respond to second messengers. Intramolecular interactions control both the accessibility of the active site to substrate and of the regulatory modules to the second messengers (Oancea and Meyer, 1998; Orr and Newton, 1994; Stensman and Larsson, 2007). PKC isozymes are critical in processing signals that drive cellular functions such as proliferation, apoptosis, and differentiation (Griner and Kazanietz, 2007; Newton, 2010). Correctly tuning PKC output is essential for cellular homeostasis and, as such, its dysregulation is associated with a myriad of diseases, including cancer, metabolic disorders, and neurodegeneration. Key to regulation of the signaling output of most PKC isozymes is the ability of cytosolic enzyme to respond to the membrane-embedded lipid second messenger, diacylglycerol (DAG), in a dynamic range that prevents signaling in the absence of agonists but allows efficient signaling in response to small changes in DAG.

PKC isozymes are classified based on their membrane-targeting domains (Newton, 2010). cPKCs (Figure 1A; PKCα, PKCβ, and PKCγ) contain tandem C1 domains (cysteine-rich zinc finger domains), that bind DAG or their functional analogs, phorbol esters (Sharkey et al., 1984), and a C2 domain that requires phosphatidylinositol-4,5-bisphosphate (PIP_2) as well as phosphatidylserine for Ca^{2+}-dependent plasma membrane targeting (Corbalan-Garcia et al., 2003; Corbin et al., 2007; Evans et al., 2006; Konig et al., 1985a). Novel PKC (nPKC) isozymes (PKCδ, PKCε, PKCη, PKCθ) also have tandem C1 domains, but lack a functional C2 domain (Cho and Stahelin, 2006). nPKCs efficiently respond to DAG production without the need for Ca^{2+}-dependent pre-targeting to the plasma membrane because their affinity for DAG is almost two orders of magnitude higher than that of cPKCs. The C2 domains of the novel PKCδ and PKCθ bind proteins containing phosphotyrosine, which for PKCθ is an activating event (Benes et al., 2005; Stahelin et al., 2012). Atypical PKCs (PKCι/λ and PKCζ) respond to neither Ca^{2+}, nor DAG, and protein scaffold interactions likely regulate their function (Kazanietz et al., 1994).

When first synthesized, PKC is in an open conformation, with its autoinhibitory pseudosubstrate out of the substrate-binding cavity (Dutil and Newton, 2000). This species of PKC is membrane-associated (Borner et al., 1989; Sonnenburg et al., 2001), but inactive. Catalytic competence requires maturation of PKC by ordered phosphorylation at three highly conserved sites: the activation loop, the turn motif, and hydrophobic motif (Newton, 2003). The first phosphorylation occurs at the activation loop by PDK-1 and positions the active site for catalysis (Dutil et al., 1998; Grodsky et al., 2006; Le Good et al., 1998). This phosphorylation triggers phosphorylation at the turn motif, which anchors the C-terminal tail onto the N-lobe of the kinase, conferring stability (Hauge et al., 2007). Turn motif phosphorylation, which is necessary for catalytic function, triggers intramolecular autophosphorylation of the hydrophobic motif (Behn-Krappa and Newton, 1999; Edwards et al., 1999). Phosphorylation at this site is not required for activity but helps align the αC helix of the kinase domain for catalysis and thus supports optimal activity and stability (Gao et al., 2008; Yang et al., 2002). Processing by phosphorylation depends on a conserved

PXXP motif (P616/P619 in PKCβII; Figure 1B) within PKC that binds the chaperone heat shock protein 90 (Gould et al., 2009); mutation of either of these Pro residues results in a kinase that is not phosphorylated and is thus inactive. Processing phosphorylations are also absent in other kinase-inactive PKC mutants, presumably because autophosphorylation is prevented (Behn-Krappa and Newton, 1999). Lastly, processing phosphorylations depend on the integrity of the mTORC2 kinase complex by an unknown mechanism (Facchinetti et al., 2008; Ikenoue et al., 2008).

Mature PKC is released to the cytosol, where it adopts an autoinhibited conformation with the pseudosubstrate bound within the substrate-binding site. Membrane engagement of the C1 and C2 domains of cPKCs, or just the C1 domain for nPKCs, induces a conformational change that expels the pseudosubstrate, activating PKC (Orr and Newton, 1994). Why PKC has two tandem C1 domains is not clear considering that only one of the C1 domains engages the membrane at a time (Kikkawa et al., 1983; Konig et al., 1985b). Several studies have shown that for the novel PKCδ, the C1B domain is the predominant membrane binding domain (Pu et al., 2009; Szallasi et al., 1996; Wu-Zhang et al., 2012). However, it remains to be elucidated which C1 domain of PKCβII is the predominant membrane binder.

Here we use fluorescence energy transfer (FRET)-based imaging to visualize conformational transitions of cPKCs and nPKCs in live cells. Using a PKC conformation reporter, Kinameleon, we show that PKCβII undergoes conformational transitions as it matures, becomes activated, and down-regulated. In addition, analysis of membrane translocation kinetics reveals that the ligand-binding surface of the C1 domains of PKC become masked during the maturation of the enzyme. This occurs through intramolecular interactions and tunes the affinity of mature PKC for optimal response to second messengers. This mechanism is commonly employed by other enzymes to optimize their dynamic range of signaling, and thus visualization of conformational rearrangements within PKC serves as a paradigm for signaling by other multi-module transducers.

Results

Maturation of cPKC retards agonist-dependent membrane translocation kinetics

We have previously shown that the integrity of a PXXP motif in PKCβII (P616/P619) is required for the proper phosphorylation and folding of PKC (Gould et al., 2009). In imaging studies co-expressing PKCβII-RFP and PKCβII-P616A/P619A-YFP in the same cell, we observed that the kinase-dead PKC translocated to the plasma membrane more rapidly than wild-type in response to phorbol dibutyrate (PDBu), a PKC agonist (Figure 1C, left panels). To determine whether this accelerated translocation was caused by lack of catalytic activity, we examined the translocation of two additional constructs whose active site had been altered to inhibit catalysis (Figure 1B). In PKCβII-K371R, the conserved Lys that coordinates the αβ phosphates of ATP was mutated (Buechler et al., 1989; Ohno et al., 1990) and in PKCβII-D466N, the conserved Asp that serves as the catalytic base in the phosphorylation reaction was mutated. This latter construct retains the ability to autophosphorylate weakly but cannot phosphorylate substrates (Gould et al., 2011; Shi et al., 2010). As observed for the PXXP mutant, both catalytically impaired constructs fully translocated to plasma membrane after 2.5 min PDBu treatment, whereas the wild-type

enzyme, in the same cell, was primarily cytosolic and required 12.5 min for membrane translocation (Figure 1B). All three kinase-dead mutants were partially localized at the plasma membrane prior to stimulation. Thus, impairing PKCβII activity by three independent mechanisms resulted in pretargeting to the plasma membrane and accelerated agonist-induced membrane translocation compared to wild-type.

To assess whether phosphorylation per se, or the ordered conformation changes that accompany maturation caused the delayed translocation kinetics of wild-type PKCβII, we evaluated the phosphorylation state of the constructs used in the translocation assays. We took advantage of the mobility shift on Western blots induced by quantitative phosphorylation at the C-terminal tail (Keranen et al., 1995). Under the conditions of our experiments, PKCβII migrated predominantly (67%) as an upper mobility band, reflecting phosphorylation at the two C-terminal priming sites (Figure 1D, lane 1, asterisk); approximately a third of the protein was not phosphorylated (lower band, dash). The kinase-inactive mutants PKCβII-K371R and PKCβII-P616A/P619A were completely unphosphorylated (Figure 1D, lanes 2 and 4). In contrast to these kinase-dead PKC mutants, the PKCβII-D466N showed equal amounts of phosphorylated (52%) and unphosphorylated (48%) species (Figure 1D, lane 3). Thus, the translocation kinetics of PKC were unrelated to the state of processing phosphorylations: wild-type PKCβII, with 67% phosphorylated species, and PKCβII-D466N, with 52% phosphorylated species, translocated with significantly different kinetics. These data reveal that the conformation of the kinase-impaired PKCβII-D466N does not recapitulate the ordered conformational transitions accompanying the maturation of wild-type PKC, despite permissive phosphorylation. In summary, catalytically-inactive constructs of PKC have accelerated membrane translocation, independently of their phosphorylation state.

Kinameleon: a probe for conformational transitions of PKC in cells

One possibility for the accelerated membrane association of kinase-inactive PKC compared with wild-type is that unprimed PKC is in a different conformation from mature PKC. To probe for conformational differences between these two species, we engineered a FRET-based conformational reporter we named Kinameleon (for the changing colors depending on conformation). Kinameleon (Figure 2A) comprises a CFP and YFP flanking the N- and C-terminus, respectively, of wild-type PKCβII (Kinameleon-WT) or the kinase-inactive PKCβII-K371R (Kinameleon-K371R). A similar approach has been used for PKCδ, and this construct was shown to behave like untagged PKCδ (Braun et al., 2005). When expressed in MDCK (Madin-Darby canine kidney) cells, unphosphorylated, kinase-dead Kinameleon-K371R, exhibited a significantly lower basal FRET ratio than mature, phosphorylated Kinameleon-WT, as illustrated by the raw pseudocolor FRET ratio image (Figure 2B). Upon 15 min stimulation with PDBu, Kinameleon-WT translocated to plasma membrane and FRET increased further, consistent with an additional conformational rearrangement upon activation. Following 12 hours PDBu treatment to promote dephosphorylation of PKC, FRET decreased to levels similar to those of Kinameleon-K371R Quantitation of the FRET ratios (FRET/CFP) as a function of time revealed that the FRET ratio for Kinameleon-WT approached that of the unprimed Kinameleon-K371R following 12 hours of PDBu stimulation (Figure 2C). The FRET increase resulted, in part, from intermolecular FRET

between Kinameleons concentrated at the plasma membrane; however, this only accounted for a small portion of the increase observed because control cells co-expressing YFP-PKCβII-YFP and CFP-PKCβII-CFP displayed a more modest increase (Figure 2D; compare upper to lower panel). These data are consistent with a model (Figure 2A) in which the N- and C-termini of PKC are oriented for low FRET in unprimed PKC, they re-orient to yield intermediate FRET upon maturation of PKC, they are repositioned for high FRET upon activation of PKC, and they regain their original orientation (low FRET) following dephosphorylation.

Translocation kinetics of isolated C1A-C1B domains of PKC can be tuned by a single residue

We have previously shown that a Trp at position 22 within the C1A or C1B domain (Figures 1B and 3A) confers an almost two orders of magnitude higher affinity for DAG than a Tyr at that position (Dries et al., 2007). In cPKCs, Trp is present in the C1A (Trp 58; high affinity for DAG) and Tyr in the C1B (Tyr 123; low affinity for DAG). Here we take advantage of this toggle to selectively tune the affinity of the C1A and/or C1B domains within cPKCs as a tool to differentiate between them. We monitored the rate of translocation of the isolated C1A-C1B domain to membranes as a function of whether Tyr or Trp was present at position 22. We used our previously developed Diacylglycerol Reporter, DAGR (Violin et al., 2003) that contains the tandem C1A-C1B domain of PKCβ flanked by CFP and YFP. Translocation of this reporter to the plasma membrane can be quantified by the increase in intermolecular FRET from CFP to YFP as the DAGR reporters become concentrated at the membrane. In response to PDBu, the isolated C1A-C1B domain translocated to the plasma membrane with a half-time of 0.82 ± 0.02 min (Figure 3B). Reducing the C1A domain's affinity for ligand by mutating Trp58 to a Tyr (C1A-C1B-W58Y) resulted in a 5-fold reduction in the rate of translocation of the C1A-C1B domain to the plasma membrane ($t_{½}$ = 3.69 ± 0.04 min) compared to wild-type. This effect could be rescued by increasing the affinity of the C1B domain for ligand: the double mutant C1A-C1B-W58Y/Y123W displayed similar translocation kinetics to wild-type. Increasing the C1B domain's affinity for ligand (C1A-C1B-Y123W) while leaving the high affinity of the C1A domain unchanged, resulted in pretargeting of the domain to the plasma membrane and Golgi (Dries et al., 2007). It was previously shown that the Y123W mutation does not perturb the structure of the C1B domain (Stewart et al., 2011), indicating that the domain is not pretargeted to membranes and unable to translocate because it is misfolded; rather its intrinsic affinity for membranes is so high that it likely binds basal levels of DAG. Moreover, the isolated C1A-C1B domain has a relatively high affinity for phorbol esters since sub-saturating levels of PDBu (50 nM) that were insufficient to maximally translocate full length PKCβII (see Figure 4D) were sufficient to cause full translocation of the C1A-C1B domain to the plasma membrane (Figure 3D). These data are consistent with the C1A and C1B moieties of the C1A-C1B module being fully accessible for membrane engagement: Tyr at the toggle position of either domain reduces the rate of translocation, whereas Trp at either position increases the rate of translocation. Moreover, constructs with Tyr in one moiety and Trp in the other moiety have similar translocation kinetics, independently of whether the Tyr is in the C1A or C1B.

Unprimed PKC has an exposed C1A-C1B domain that is masked upon proper maturation

Using FRET, we quantified the translocation kinetics of YFP-tagged cPKCs towards plasma membrane-targeted CFP. PKCβII translocated to the plasma membrane in response to PDBu with significantly slower kinetics than the isolated C1A-C1B domain (Figure 4A; t½ = 3.56 ± 0.02 min versus 0.82 ± 0.02 min). In contrast, the unphosphorylated PKCβII-K371R and PKCβII-P616A/P619A mutants translocated with rates that matched those of the isolated C1A-C1B domain (t½ = 0.35 ± 0.07 min and t½ = 0.63 ± 0.05 min, respectively). These data are consistent with both C1A and C1B moieties being fully exposed in these mutants, whereas one or the other (or both) becomes masked in the properly primed wild-type PKCβII. PKCβII-D466N (t½ = 0.53 ± 0.07 min) also translocated with kinetics similar to those of the isolated C1A-C1B domain, suggesting that even though about 52% of the pool of PKCβII-D466N is phosphorylated, it is not properly folded. Next we examined whether the C1A-C1B domain of another cPKC, PKCα, was also masked during maturation. The corresponding PKCα kinase-dead mutant, PKCα-K368M, migrated as an unphosphorylated species on a PAGE gel (Figure 4B, lanes 2 and 4, dash) whereas 52% of the pool of PKCα-D463N was phosphorylated at the C-terminal sites (Figure 4B, compare lanes 1 and 3), same as for PKCβII-D466N. Yet both of these kinase-dead PKCα mutants (PKCα-K368M t½ = 0.82 ± 0.02 min; PKCα-D463N t½ = 1.26 ± 0.01 min) responded more rapidly to PDBu than wild-type (t½ = 9.18 ± 0.01 min) (Figure 4C), showing that the trend of fast translocation of kinase-dead PKCs is a common phenomenon among cPKCs. These data corroborate that the kinase-dead PKCβII-D466N and PKCα-D463N do not adopt the conformation of wild-type enzyme despite being partially phosphorylated. Thus, cPKCs undergo a conformational change upon proper PKC maturation, which masks the ligand-binding surface of the C1A-C1B domain, leading to a slower translocation of primed PKC compared to unprocessed PKC or to the isolated C1A-C1B domain.

As an additional measure of whether the C1A-C1B domain becomes masked upon maturation we examined membrane binding induced by sub-saturating concentrations of phorbol esters (50nM). Whereas the C1A-C1B domain fully translocated to the plasma membrane upon 50 nM PDBu, less than 50% of the pool of monitored full-length, wild-type PKCβII translocated (Figure 4C compared to Figure 3D). However, all the kinase-dead PKCβIIs maximally translocated, (Figure 3D), suggesting that these unprimed or improperly primed mutants have a lower threshold for PDBu activation resulting from fully exposed ligand-binding surfaces on their C1A-C1B domains.

Both the C1A and C1B domains of unphosphorylated PKC are exposed and become masked upon priming

Conventional and novel PKCs have two functional C1 domains, yet only one of the domains is engaged on the membrane at a time (Giorgione et al., 2003; Kikkawa et al., 1983). To dissect the respective contribution of each domain on driving translocation of PKCβII, we addressed the effect of altering the ligand affinity of the C1A and C1B domains on ligand-dependent membrane translocation. We first examined the phorbol ester-dependent membrane translocation, and then the DAG-dependent translocation (see below), as the differences in affinity for these two ligands vary greatly between the domains. Specifically, the affinity of the C1A domain for DAG is almost two orders of magnitude higher than that

of the C1B domain, whereas for PDBu, the difference in affinity is only 6-fold (Dries et al., 2007). To this end, we altered the affinity of the C1A or C1B domain by mutating the residue at position 22 within full-length PKCβII. A Trp to Tyr mutation in the C1A domain (PKCβII-W58Y) did not affect translocation kinetics (Figure 5A), which consistent with the ligand-binding surface of the C1A domain being occluded within primed PKCβII. In contrast, the translocation kinetics of the kinase-dead PKCβII-W58Y/K371R (Figure 5B; t½ = 1.38 ± 0.04 versus 0.35 ± 0.07 min) and PKCβII-W58Y/D466N (Figure 5C; t½ = 1.55 ± 0.04 versus 0.52 ± 0.04 min) were sensitive to mutation of the C1A domain, revealing that the C1A domain is exposed in these mutants. To further show that this single residue can dictate the translocation kinetics of full-length kinase-dead PKC, we inverted the DAG affinities of the C1A (from high to low) and C1B domains (from low to high) in a kinase inactive construct. This PKCβII-W58Y/Y123W/D466N mutant translocated with similar kinetics to that of PKCβII-D466N (Figure 5C; t½ = 0.49 ± 0.06 min vs. 0.52 ± 0.04 min), supporting the finding that both domains are exposed in this improperly processed PKC and revealing that these mutations do not affect the folding of the C1 domains. Moreover, these results show that it does not matter whether the higher affinity domain is positioned before or after the lower affinity domain. Curiously, the PKCβII-W58Y/P616A/P619A (0.71 ± 0.03 min) mutant did not display slower kinetics of translocation than PKCβII-P616A/P619A (0.63 ± 0.05 min) (Figure 5D), suggesting that this mutant may be folded differently from the other kinase-inactive ones. These data reveal that the ligand-binding surface of both C1A and C1B domains are exposed in unprocessed PKC and that the C1A domain becomes occluded during maturation.

We next addressed whether the C1B domain is exposed in matured PKCβII. There was no difference between PKCβII and PKCβII-Y123W (Figure 5A), indicating that the ligand-binding surface of the C1B domain is also masked in the fully matured PKC. However, the C1B domain is fully exposed in the kinase dead mutants, as evidenced by the mutants constitutive association with the plasma membrane and the Golgi (Figure 5E, top panels), similarly to the C1A-C1B-Y123W domain mutant (Figure 3C). These mutants displayed no further translocation to the plasma membrane with PDBu treatment (Figure 5E, bottom panels).

To further validate that both the C1A and C1B domains are exposed in unprocessed PKC, we examined the effect of preventing processing of the novel PKCδ, which contains two high-affinity C1 domains as it has Trp at position 22 in both domains (Figure 1A). The kinase-dead PKCδ-K376R and PKCδ-D471N were constitutively associated with the plasma membrane and Golgi (Figure 5E), consistent with exposure of two high affinity DAG binders causing constitutive membrane interaction. These data reveal that unprimed mutants of both conventional and novel PKCs have exposed ligand-binding surfaces in their C1A and C1B domains and that these surfaces become occluded through intramolecular conformational changes as PKC matures.

Both the C1A and C1B domains are involved in membrane binding, but the C1B domain dominates

The insensitivity of mature PKC towards changes in ligand affinity of the C1A or C1B domain toward PDBu could reflect the use of saturating concentrations of this potent ligand, such that 6-fold differences in ligand affinity between Trp versus Tyr at position 22 might be undetectable. To address this, we used a much lower affinity ligand, DAG, to test whether stimulation with sub-saturating levels of the synthetic DAG, 1,2-Dioctanoyl-sn-glycerol (DiC8) could reveal a difference between PKCβII and PKCβII in which the affinity of either the C1A or C1B domain has been altered. Modifying the affinity of either the C1A or C1B domain altered the steady-state levels of PKCβII bound to the DiC8-containing plasma membrane (and thus the amplitude of translocation): decreasing the affinity of the C1A domain (PKCβII-W58Y) lowered the amplitude of translocation by 13%, whereas increasing the affinity of the C1B domain (PKCβII-Y123W) increased the amplitude by 20% (Figure 6). In comparison, the unprimed PKCβII-D466N mutant translocated maximally and with much faster kinetics than wild-type enzyme upon DiC8 treatment, reflecting two highly exposed C1 domains. These data further sustain that properly primed PKCβII has its ligand-binding surfaces on both its C1A and C1B domains masked and that the improperly primed PKCβII-D466N mutant's translocation does not mimic that of WT PKCβII.

Discussion

Here we use genetically-encoded reporters to show that maturation of PKCβII by phosphorylation triggers conformational changes that set the ligand affinity of the enzyme for optimal signaling. The paradigm of intramolecular interactions tuning the ligand binding affinity to increase the dynamic range of a signaling molecule is employed by numerous multi-domain enzymes. For example, the Src family of tyrosine kinases displays intramolecular interactions between its kinase domain and its phospho-Tyr binding SH2 domain and PXXP-recognizing SH3 domain to maintain the kinase in an inactive conformation (Boggon and Eck, 2004; Hof et al., 1998). In this case, the enzyme's affinity for its domains is sufficiently low to allow intermolecular ligands to effectively compete and allow signal transduction. Similarly, intramolecular interactions of the PH and Ras-association domains of the Rap1-interacting adapter molecule restrain their ability to bind membranes (Wynne et al., 2012). This also seems to be the case for the PH domain of Akt (Astoul et al., 1999), consistent with intramolecular interactions lowering the affinity of its PH domain for membranes to optimize its signaling.

Extensive studies have established that PKC is matured by phosphorylation, but the role of phosphorylation in structuring the enzyme for signaling is not known. Partial crystal structures of PKC have been solved (Grodsky et al., 2006; Guerrero-Valero et al., 2009; Leonard et al., 2011; Xu et al., 1997); however, little information exists on conformational rearrangements. Using Kinameleon, we show that unprocessed PKC and PKC that has been dephosphorylated following prolonged activation are both in an open conformation that is distinct from the closed conformation of mature, but inactive, PKC. Analysis of translocation kinetics reveal that the ligand-binding surfaces of the C1A and C1B domains

are fully exposed in this open conformation but become masked upon maturation by phosphorylation. Our data are consistent with the partial PKCβII structure, which shows that phosphorylation anchors the carboxyl-terminal tail of PKC onto the top of its N-lobe where it interacts with the C1B domain (Leonard et al., 2011), preventing this domain from easily accessing DAG. Our data also corroborate work from Larsson and colleagues showing that the membrane translocation of kinase-dead PKCα-K368M is much more sensitive to DAG than wild-type PKCα (Stensman et al., 2004). They propose that only the C1A domain of PKCα is masked through intramolecular interaction between the C-terminal tail and the C2 domain (Stensman and Larsson, 2007), whereas our data are more consistent with both C1A and C1B domains of PKCβII becoming masked. This masking of the C1 domains likely occurs in all cPKCs and some of the nPKCs; the C1 domains of PKCγ were also shown to be occluded in the full length protein (Oancea and Meyer, 1998) and here we show PKCδ's C1 domains are also masked, consistent with a study by Stahelin et al. (Stahelin et al., 2004). We also demonstrate that species of PKC with impaired catalytic activity remain in the open conformation regardless of phosphorylation status: although half of the pool of PKCβII-D466N or PKCα-D463N is phosphorylated, the translocation kinetics of these kinase-dead mutants are identical to those of the isolated C1A-C1B domain, not those of wild-type PKC, suggesting that these kinase-inactive PKCs are not folded like wild-type PKC. We note caution should be taken when using kinase-dead mutants because they do not provide the same scaffolding structure as wild-type, their translocation is much more sensitive to DAG and, in the case of nPKCs, they are localized differently from wild-type, a finding consistent with work from the Steinberg lab (Guo et al., 2010). It is also noteworthy that gross overexpression of PKC allows a pool of PKC to remain unprocessed and thus more readily associate with membranes. In summary, our data are consistent with a model in which phosphorylation triggers a series of ordered conformational transitions, by a mechanism that requires the intrinsic catalytic activity of PKC, that masks the C1 domains such that the lower affinity DAG sensor, the C1B domain, is used for PKCβII.

The stoichiometry of ligand binding of full length PKC is one mole DAG/phorbol ester per mole PKC (Kikkawa et al., 1983; Konig et al., 1985b), and kinetic studies have established that there is no cooperativity in binding DAG (Hill coefficient = 1), as would be expected from the reduction in dimensionality of engaging the second C1 domain once the first one has engaged on the membrane (Hannun and Bell, 1986; Mosior and Newton, 1998; Newton and Koshland, 1989). Yet whether the C1A or C1B dominates as the DAG sensor in PKCβII has not been well established. To distinguish between the contributions of these domains, we engineered PKCβII mutants in which we toggled the affinity of each C1 domains for ligand. Inverting the affinities of the C1A and C1B domains for ligand had no apparent effect on PDBu-induced PKC translocation rates (Figure 5A), likely because this switch has a modest effect on phorbol ester binding and because saturating concentrations of PDBu were used. Importantly, stimulation with sub-saturating levels of DAG, which exhibits an almost two orders of magnitude higher affinity for the C1A versus C1B domain (Dries et al., 2007), uncovered a difference (Figure 6). Decreasing the affinity of the C1A domain for ligand lowered the steady-state levels of PKCpII bound to the plasma membrane, whereas increasing the affinity of the C1B domain increased the steady-state levels bound to the membrane, suggesting that both domains can be involved in membrane binding. The altered

membrane affinities are likely caused by changes in the membrane dissociation rate, as we have previously shown that mutants with lower affinities for DAG have increased membrane dissociation rate constants (Dries and Newton, 2008). However, reducing the affinity of the C1A domain for DAG by almost 100-fold only decreased steady-state binding by two-fold. If this were the dominant binding domain, the steady-state levels should have decreased by at least an order of magnitude more. This suggests that the C1B is the predominant binding domain for PKCβII. Here, increasing the membrane affinity by 100-fold increased steady-state levels also by two-fold; this is less than expected but consistent with the C1B domain being masked in the full-length wild-type enzyme. Moreover, our data show that both the C1A and C1B domains are exposed in kinase-dead PKCs, because toggling the affinity of either domain had a significant effect on their translocation kinetics.

Based on these studies on PKC conformation, we build on the model for PKC maturation (Figure 7). We propose that unprimed PKC is in an open conformation that associates with membranes (Sonnenburg et al, 2001) through weak interactions with the pseudosubstrate (Mosior and McLaughlin, 1991), C1 and C2 domains (Johnson et al, 2000), and C-terminal tail (Yang and Igumenova, 2013). Both the C1A and C1B domains are exposed and the pseudosubstrate is out of the active site (Dutil and Newton, 2000; Johnson et al., 2000) (Figure 7A). Upon ordered phosphorylation of PKC at its three priming sites, PKC matures into its closed conformation in which the ligand-binding surface of both the C1A and C1B domains becomes masked and the pseudosubstrate occupies the substrate-binding cavity (Figure 7B). Thus PKCs are maintained in an inactive, closed conformation by intramolecular interactions induced by phosphorylation. Upon activation, cPKCs translocate to membranes by a two-step mechanism (Nalefski and Newton, 2001): first, binding of Ca^{2+} to the C2 domain mediates its binding to the membrane through electrostatic and hydrophobic interactions (Scott et al., 2013) (Figure 7C). Since the C2 domain of cPKC has a high affinity for PIP_2, which is enriched within the plasma membrane compared to other membranes, cPKCs preferentially translocate to this membrane (Evans et al., 2006; Ferrer-Orta et al., 2009; Guerrero-Valero et al., 2009; Marin-Vicente et al., 2005). Engagement of the C2 domain in the membrane not only reduces the dimensionality of the C1A or C1B domain search for DAG, but also leads to intramolecular conformational changes (Stahelin and Cho, 2001) that allow the C1A and C1B domains to become slightly more exposed (Bittova et al., 2001). Secondly, binding of either the C1A or the C1B domain, but predominantly the C1B domain for PKCβII (Figure 7D), to DAG, expels the pseudosubstrate and activates PKC. Use of this lower affinity C1B domain as the primary membrane localization module for cPKCs allows PKC to respond accordingly to a wider range of DAG levels at the plasma membrane. Upon activation, PKC is quickly dephosphorylated and thus transitions back to its exposed (open) conformation of unprimed PKC (Figure 7E).

In summary, our data reveal an elegant mechanism by which intramolecular conformational transitions tune the affinity of mature PKC for its allosteric activator, DAG, as a regulatory mechanism to allow ultrasensitivity in the signaling output of PKC. We have previously shown that the binding of PKC to membranes displays high cooperativity with respect to phosphatidylserine (Newton and Koshland, 1989; Orr and Newton, 1992). Thus, by reducing the affinity of both conventional and novel PKCs for membranes through conformational

transitions induced during maturation, basal signaling of these isozymes is minimized. Indeed, without this masking by maturation, isozymes such as the novel PKCδ that has two high affinity C1 domains would be constitutively pretargeted to the plasma membrane and the Golgi; for these isozymes, masking of the C1 domains is necessary to prevent constitutive association of PKC with membranes and thus constitutive activity. The mature enzyme conformation does, however, enable PKCs to respond effectively to very small changes in DAG. Moreover, basal signaling of PKCβII is further attenuated through the preferential use of the lower affinity DAG sensor, the C1B domain, which allows cPKCs to signal at different membranes from nPKCs. The affinity of the C1B domain for DAG is too low to allow cPKCs to sense agonist-evoked changes in this second messenger without pre-targeting by the Ca^{2+}-regulated C2 domain (Dries et al., 2007); therefore, cPKCs are directed to the plasma membrane via the PIP_2-sensing C2 domain where they can then find DAG. In contrast, nPKCs, which have a higher affinity C1B domain, translocate to the most DAG-enriched membrane, the Golgi, without the need for pre-targeting. Thus, masking of the C1A domain in cPKCs tunes the affinity of PKC to reduce basal signaling, increase the dynamic range of the PKC signal, and determine the membrane to which PKC is recruited.

Significance

In this manuscript, we follow conformational transitions in living cells to unveil a key regulatory mechanism in cell signaling: tuning of ligand affinity by intramolecular conformational changes. Specifically, we use FRET-based reporters, in live cells, to show how a multi-domain signal transducer, PKC, undergoes conformational transitions upon phosphorylation-induced maturation that tune the affinity of its DAG-binding C1A and C1B domains for optimal signaling. Importantly, we show that these conformational transitions keep PKC inactive under basal conditions, but allow ultrasensitivity in responses to small changes in agonist-evoked levels of DAG. Conformational rearrangements that optimize the dynamic range of signaling will likely serve as a paradigm for signaling by many other multi-module transducers. Our FRET-based methods to visualize these changes in living cells are applicable to the vast array of multi-module signal transducers.

Experimental Procedures

Plasmid Constructs

C-terminally tagged rat PKCβII-YFP (Dries et al, 2007), rat PKCβII-RFP (Gould et al., 2009), mouse PKCδ-YFP (Wu-Zhang et al., 2012), DAGR, bovine PKCα-HA, and membrane-targeted CFP were described previously (Violin et al., 2003). Kinameleon was cloned into pcDNA3 as YFP-PKCβII-CFP and Kinameleon-K371R was generated by QuikChange site-directed mutagenesis (Stratagene). A C1A-C1B construct containing the N-terminus of rat PKCβII (residues 1-156) was subcloned into DAGR. Bovine YFP-PKCα was generated by subcloning PKCα into pcDNA3 with YFP at the N-terminus. All mutants were generated by QuikChange site-directed mutagenesis (Stratagene).

Antibodies and Materials

The mouse monoclonal anti-HA antibody (HA.11, clone 16B12) was purchased from Covance, the mouse monoclonal anti-β-actin antibody (A2228) was purchased from Sigma-Aldrich, and the mouse monoclonal anti-PKCβ antibody (610128) was from BD Transduction Laboratories. Phorbol 12,13-dibutyrate (PDBu) and 1,2-Dioctanoyl-sn-glycerol (DiC8) were obtained from Calbiochem. The 1X Hanks' Balanced Salt Solution was purchased from Cellgro. All other materials and chemicals were reagent grade.

Cell Culture, Transfection, and Immunoblotting

COS7 cells were maintained in DMEM (Cellgro) containing 5% or 10% fetal bovine serum (Gibco) and 1% penicillin/streptomycin (Gibco) at 37 °C in 5% CO_2. MDCK cells were cultured in DMEMF-12 50/50 (Cellgro) containing 10% FBS and 1% penicillin/streptomycin. Transient transfection of COS7 was carried out using the jetPRIME transfection reagent (PolyPlus Transfection) or the FuGENE 6 transfection reagent (Roche Applied Science) for ~24h. MDCK cells were transiently transected using PolyFect (Qiagen) for ~36h. Cells were lysed in 50 mM Tris, pH 7.4, 1% Triton X-100, 50 mM NaF, 10 mM $Na_4P_2O_7$, 100 mM NaCl, 5 mM EDTA, 1 mM Na_3VO_4, 1 mM PMSF, and 50 nM Okadaic acid. Whole cell lysates were analyzed by SDS-PAGE and Western blotting via chemiluminescence on a FluorChem imaging system (Alpha Innotech).

FRET Imaging and Analysis

Cells were plated onto glass coverslips in 35 mm dishes, transfected with the indicated constructs, and imaged in Hanks' Balanced Salt Solution supplemented with 1 mM $CaCl_2$. CFP, YFP, and FRET images were acquired with a 40X objective with a Zeiss Axiovert microscope (Carl Zeiss Microimaging) using a MicroMax digital camera (Roper-Princeton Instruments) controlled by MetaFluor software version 6.1r6 (Universal Imaging Corporation) as described previously (Gallegos et al., 2006). Pseudocolor images were acquired at the indicated times before and after treatment with 200 nM PDBu and normalized to the same min and max values. For the translocation experiments, base-line images were acquired every 7 or 15 sec for 3 or more min before ligand addition. Because the maximal amplitude of translocation of the mutants varied, possibly due to changes in the orientation or distance of the fluorophores caused by differential folding of the kinase, the data were normalized to the maximal amplitude of translocation for each cell. Normalization was achieved by dividing by the average base-line FRET ratio, and then scaled from 0 to 100 % of maximal translocation using the equation: $X = (Y-Y_{min})/(Y_{max}-Y_{min})$, where Y = normalized FRET ratio, Y_{min} = minimum value of Y, and Y_{max} is maximum value of Y. Data from at least three different imaging dishes were referenced around the ligand addition time point and the average of these normalized values ± SEM were plotted and curve fitted. Curve fitting was performed using Graph Pad Prism 6.0a (GraphPad Software Inc., CA, USA). The half-time of translocation was calculated by fitting the data to a non-linear regression using a one-phase exponential association equation.

Acknowledgments

We thank Alyssa Wu-Zhang, Emily Kang, and Timothy R. Baffi for technical assistance. This work was supported by NIH GM43154 to ACN. CEA and JDV were supported in part by the UCSD Graduate Training Program in Cellular and Molecular Pharmacology (T32 GM007752). CEA was supported in part by the NSF Graduate Research Fellowship (DGE1144086).

References

Astoul E, Watton S, Cantrell D. The dynamics of protein kinase B regulation during B cell antigen receptor engagement. J Cell Biol. 1999; 145:1511–1520. [PubMed: 10385529]

Behn-Krappa A, Newton AC. The hydrophobic phosphorylation motif of conventional protein kinase C is regulated by autophosphorylation. Curr Biol. 1999; 9:728–737. [PubMed: 10421574]

Benes CH, Wu N, Elia AE, Dharia T, Cantley LC, Soltoff SP. The C2 domain of PKCdelta is a phosphotyrosine binding domain. Cell. 2005; 121:271–280. [PubMed: 15851033]

Bittova L, Stahelin RV, Cho W. Roles of ionic residues of the C1 domain in protein kinase C-alpha activation and the origin of phosphatidylserine specificity. J Biol Chem. 2001; 276:4218–4226. [PubMed: 11029472]

Boggon TJ, Eck MJ. Structure and regulation of Src family kinases. Oncogene. 2004; 23:7918–7927. [PubMed: 15489910]

Borner C, Filipuzzi I, Wartmann M, Eppenberger U, Fabbro D. Biosynthesis and posttranslational modifications of protein kinase C in human breast cancer cells. J Biol Chem. 1989; 264:13902–13909. [PubMed: 2474538]

Braun DC, Garfield SH, Blumberg PM. Analysis by fluorescence resonance energy transfer of the interaction between ligands and protein kinase Cdelta in the intact cell. J Biol Chem. 2005; 280:8164–8171. [PubMed: 15611119]

Buechler JA, Vedvick TA, Taylor SS. Differential labeling of the catalytic subunit of cAMP-dependent protein kinase with acetic anhydride: substrate-induced conformational changes. Biochemistry. 1989; 28:3018–3024. [PubMed: 2500968]

Cho W, Stahelin RV. Membrane binding and subcellular targeting of C2 domains. Biochimica et biophysica acta. 2006; 1761:838–849. [PubMed: 16945584]

Corbalan-Garcia S, Garcia-Garcia J, Rodriguez-Alfaro JA, Gomez-Fernandez JC. A new phosphatidylinositol 4,5-bisphosphate-binding site located in the C2 domain of protein kinase Calpha. J Biol Chem. 2003; 278:4972–4980. [PubMed: 12426311]

Corbin JA, Evans JH, Landgraf KE, Falke JJ. Mechanism of specific membrane targeting by C2 domains: localized pools of target lipids enhance Ca2+ affinity. Biochemistry. 2007; 46:4322–4336. [PubMed: 17367165]

Dries DR, Gallegos LL, Newton AC. A single residue in the C1 domain sensitizes novel protein kinase C isoforms to cellular diacylglycerol production. J Biol Chem. 2007; 282:826–830. [PubMed: 17071619]

Dries DR, Newton AC. Kinetic analysis of the interaction of the C1 domain of protein kinase C with lipid membranes by stopped-flow spectroscopy. J Biol Chem. 2008; 283:7885–7893. [PubMed: 18187412]

Dutil EM, Newton AC. Dual role of pseudosubstrate in the coordinated regulation of protein kinase C by phosphorylation and diacylglycerol. J Biol Chem. 2000; 275:10697–10701. [PubMed: 10744767]

Dutil EM, Toker A, Newton AC. Regulation of conventional protein kinase C isozymes by phosphoinositide-dependent kinase 1 (PDK-1). Curr Biol. 1998; 8:1366–1375. [PubMed: 9889098]

Edwards AS, Faux MC, Scott JD, Newton AC. Carboxyl-terminal phosphorylation regulates the function and subcellular localization of protein kinase C betaII. J Biol Chem. 1999; 274:6461–6468. [PubMed: 10037738]

Evans JH, Murray D, Leslie CC, Falke JJ. Specific translocation of protein kinase Calpha to the plasma membrane requires both Ca2+ and PIP2 recognition by its C2 domain. Molecular biology of the cell. 2006; 17:56–66. [PubMed: 16236797]

Facchinetti V, Ouyang W, Wei H, Soto N, Lazorchak A, Gould C, Lowry C, Newton AC, Mao Y, Miao RQ, et al. The mammalian target of rapamycin complex 2 controls folding and stability of Akt and protein kinase C. The EMBO journal. 2008; 27:1932–1943. [PubMed: 18566586]

Ferrer-Orta C, Agudo R, Domingo E, Verdaguer N. Structural insights into replication initiation and elongation processes by the FMDV RNA-dependent RNA polymerase. Current opinion in structural biology. 2009; 19:752–758. [PubMed: 19914060]

Gallegos LL, Kunkel MT, Newton AC. Targeting protein kinase C activity reporter to discrete intracellular regions reveals spatiotemporal differences in agonist-dependent signaling. J Biol Chem. 2006; 281:30947–30956. [PubMed: 16901905]

Gao T, Brognard J, Newton AC. The phosphatase PHLPP controls the cellular levels of protein kinase C. J Biol Chem. 2008; 283:6300–6311. [PubMed: 18162466]

Giorgione J, Hysell M, Harvey DF, Newton AC. Contribution of the C1A and C1B domains to the membrane interaction of protein kinase C. Biochemistry. 2003; 42:11194–11202. [PubMed: 14503869]

Gould CM, Antal CE, Reyes G, Kunkel MT, Adams RA, Ziyar A, Riveros T, Newton AC. Active site inhibitors protect protein kinase C from dephosphorylation and stabilize its mature form. J Biol Chem. 2011; 286:28922–28930. [PubMed: 21715334]

Gould CM, Kannan N, Taylor SS, Newton AC. The chaperones Hsp90 and Cdc37 mediate the maturation and stabilization of protein kinase C through a conserved PXXP motif in the C-terminal tail. J Biol Chem. 2009; 284:4921–4935. [PubMed: 19091746]

Griner EM, Kazanietz MG. Protein kinase C and other diacylglycerol effectors in cancer. Nat Rev Cancer. 2007; 7:281–294. [PubMed: 17384583]

Grodsky N, Li Y, Bouzida D, Love R, Jensen J, Nodes B, Nonomiya J, Grant S. Structure of the catalytic domain of human protein kinase C beta II complexed with a bisindolylmaleimide inhibitor. Biochemistry. 2006; 45:13970–13981. [PubMed: 17115692]

Guerrero-Valero M, Ferrer-Orta C, Querol-Audi J, Marin-Vicente C, Fita I, Gomez-Fernandez JC, Verdaguer N, Corbalan-Garcia S. Structural and mechanistic insights into the association of PKCalpha-C2 domain to PtdIns(4,5)P2. Proceedings of the National Academy of Sciences of the United States of America. 2009; 106:6603–6607. [PubMed: 19346474]

Guo J, Cong L, Rybin VO, Gertsberg Z, Steinberg SF. Protein kinase C-{delta} regulates the subcellular localization of Shc in H2O2-treated cardiomyocytes. American journal of physiology Cell physiology. 2010; 299:C770–778. [PubMed: 20686066]

Hannun YA, Bell RM. Phorbol ester binding and activation of protein kinase C on triton X-100 mixed micelles containing phosphatidylserine. J Biol Chem. 1986; 261:9341–9347. [PubMed: 3459728]

Hauge C, Antal TL, Hirschberg D, Doehn U, Thorup K, Idrissova L, Hansen K, Jensen ON, Jorgensen TJ, Biondi RM, et al. Mechanism for activation of the growth factor-activated AGC kinases by turn motif phosphorylation. The EMBO journal. 2007; 26:2251–2261. [PubMed: 17446865]

Hof P, Pluskey S, Dhe-Paganon S, Eck MJ, Shoelson SE. Crystal structure of the tyrosine phosphatase SHP-2. Cell. 1998; 92:441–450. [PubMed: 9491886]

Ikenoue T, Inoki K, Yang Q, Zhou X, Guan KL. Essential function of TORC2 in PKC and Akt turn motif phosphorylation, maturation and signalling. The EMBO journal. 2008; 27:1919–1931. [PubMed: 18566587]

Johnson JE, Giorgione J, Newton AC. The C1 and C2 domains of protein kinase C are independent membrane targeting modules, with specificity for phosphatidylserine conferred by the C1 domain. Biochemistry. 2000; 39:11360–11369. [PubMed: 10985781]

Kazanietz MG, Bustelo XR, Barbacid M, Kolch W, Mischak H, Wong G, Pettit GR, Bruns JD, Blumberg PM. Zinc finger domains and phorbol ester pharmacophore. Analysis of binding to mutated form of protein kinase C zeta and the vav and c-raf proto-oncogene products. J Biol Chem. 1994; 269:11590–11594. [PubMed: 8157692]

Keranen LM, Dutil EM, Newton AC. Protein kinase C is regulated in vivo by three functionally distinct phosphorylations. Curr Biol. 1995; 5:1394–1403. [PubMed: 8749392]

Kikkawa U, Takai Y, Tanaka Y, Miyake R, Nishizuka Y. Protein kinase C as a possible receptor protein of tumor-promoting phorbol esters. J Biol Chem. 1983; 258:11442–11445. [PubMed: 6311812]

Konig B, Di Nitto PA, Blumberg PM. Phospholipid and Ca++ dependency of phorbol ester receptors. Journal of cellular biochemistry. 1985a; 27:255–265. [PubMed: 3157693]

Konig B, DiNitto PA, Blumberg PM. Stoichiometric binding of diacylglycerol to the phorbol ester receptor. Journal of cellular biochemistry. 1985b; 29:37–44. [PubMed: 4055921]

Le Good JA, Ziegler WH, Parekh DB, Alessi DR, Cohen P, Parker PJ. Protein kinase C isotypes controlled by phosphoinositide 3-kinase through the protein kinase PDK1. Science. 1998; 281:2042–2045. [PubMed: 9748166]

Leonard TA, Rozycki B, Saidi LF, Hummer G, Hurley JH. Crystal structure and allosteric activation of protein kinase C betaII. Cell. 2011; 144:55–66. [PubMed: 21215369]

Marin-Vicente C, Gomez-Fernandez JC, Corbalan-Garcia S. The ATP-dependent membrane localization of protein kinase Calpha is regulated by Ca2+ influx and phosphatidylinositol 4,5-bisphosphate in differentiated PC12 cells. Molecular biology of the cell. 2005; 16:2848–2861. [PubMed: 15814842]

Mosior M, McLaughlin S. Peptides that mimic the pseudosubstrate region of protein kinase C bind to acidic lipids in membranes. Biophysical journal. 1991; 60:149–159. [PubMed: 1883933]

Mosior M, Newton AC. Mechanism of the apparent cooperativity in the interaction of protein kinase C with phosphatidylserine. Biochemistry. 1998; 37:17271–17279. [PubMed: 9860841]

Nalefski EA, Newton AC. Membrane binding kinetics of protein kinase C betaII mediated by the C2 domain. Biochemistry. 2001; 40:13216–13229. [PubMed: 11683630]

Newton A. Protein kinase C: poised to signal. American journal of physiology Endocrinology and metabolism. 2010; 298:402.

Newton AC. Regulation of the ABC kinases by phosphorylation: protein kinase C as a paradigm. Biochem J. 2003; 370:361–371. [PubMed: 12495431]

Newton AC, Koshland DE Jr. High cooperativity, specificity, and multiplicity in the protein kinase C-lipid interaction. J Biol Chem. 1989; 264:14909–14915. [PubMed: 2768246]

Oancea E, Meyer T. Protein Kinase C as a Molecular Machine for Decoding Calcium and Diacylglycerol Signals. Cell. 1998; 95:307–318. [PubMed: 9814702]

Ohno S, Konno Y, Akita Y, Yano A, Suzuki K. A point mutation at the putative ATP-binding site of protein kinase C alpha abolishes the kinase activity and renders it down-regulation-insensitive. A molecular link between autophosphorylation and down-regulation. J Biol Chem. 1990; 265:6296–6300. [PubMed: 2318854]

Orr JW, Newton AC. Interaction of protein kinase C with phosphatidylserine. 1. Cooperativity in lipid binding. Biochemistry. 1992; 31:4661–4667. [PubMed: 1581316]

Orr JW, Newton AC. Intrapeptide regulation of protein kinase C. J Biol Chem. 1994; 269:8383–8387. [PubMed: 8132562]

Pawson T. Protein modules and signalling networks. Nature. 1995; 373:573–580. [PubMed: 7531822]

Pawson T. Dynamic control of signaling by modular adaptor proteins. Current opinion in cell biology. 2007; 19:112–116. [PubMed: 17317137]

Pu Y, Garfield SH, Kedei N, Blumberg PM. Characterization of the differential roles of the twin C1a and C1b domains of protein kinase C-delta. J Biol Chem. 2009; 284:1302–1312. [PubMed: 19001377]

Scott AM, Antal CE, Newton AC. Electrostatic and Hydrophobic Interactions Differentially Tune Membrane Binding Kinetics of the C2 Domain of Protein Kinase Calpha. J Biol Chem. 2013

Sharkey NA, Leach KL, Blumberg PM. Competitive inhibition by diacylglycerol of specific phorbol ester binding. Proceedings of the National Academy of Sciences of the United States of America. 1984; 81:607–610. [PubMed: 6320198]

Shi F, Telesco SE, Liu Y, Radhakrishnan R, Lemmon MA. ErbB3/HER3 intracellular domain is competent to bind ATP and catalyze autophosphorylation. Proceedings of the National Academy of Sciences of the United States of America. 2010; 107:7692–7697. [PubMed: 20351256]

Sonnenburg ED, Gao T, Newton AC. The Phosphoinositide-dependent Kinase, PDK-1, Phosphorylates Conventional Protein Kinase C Isozymes by a Mechanism That Is Independent of Phosphoinositide 3-Kinase. Journal of Biological Chemistry. 2001; 276:45289–45297. [PubMed: 11579098]

Stahelin RV, Cho W. Roles of calcium ions in the membrane binding of C2 domains. Biochem J. 2001; 359:679–685. [PubMed: 11672443]

Stahelin RV, Digman MA, Medkova M, Ananthanarayanan B, Rafter JD, Melowic HR, Cho W. Mechanism of diacylglycerol-induced membrane targeting and activation of protein kinase Cdelta. J Biol Chem. 2004; 279:29501–29512. [PubMed: 15105418]

Stahelin RV, Kong KF, Raha S, Tian W, Melowic HR, Ward KE, Murray D, Altman A, Cho W. Protein kinase Ctheta C2 domain is a phosphotyrosine binding module that plays a key role in its activation. J Biol Chem. 2012; 287:30518–30528. [PubMed: 22787157]

Stensman H, Larsson C. Identification of acidic amino acid residues in the protein kinase C alpha V5 domain that contribute to its insensitivity to diacylglycerol. J Biol Chem. 2007; 282:28627–28638. [PubMed: 17673466]

Stensman H, Raghunath A, Larsson C. Autophosphorylation suppresses whereas kinase inhibition augments the translocation of protein kinase Calpha in response to diacylglycerol. J Biol Chem. 2004; 279:40576–40583. [PubMed: 15277524]

Stewart MD, Morgan B, Massi F, Igumenova TI. Probing the determinants of diacylglycerol binding affinity in the C1B domain of protein kinase Calpha. Journal of molecular biology. 2011; 408:949–970. [PubMed: 21419781]

Szallasi Z, Bogi K, Gohari S, Biro T, Acs P, Blumberg PM. Non-equivalent roles for the first and second zinc fingers of protein kinase Cdelta. Effect of their mutation on phorbol ester-induced translocation in NIH 3T3 cells. J Biol Chem. 1996; 271:18299–18301. [PubMed: 8702464]

Violin JD, Zhang J, Tsien RY, Newton AC. A genetically encoded fluorescent reporter reveals oscillatory phosphorylation by protein kinase C. J Cell Biol. 2003; 161:899–909. [PubMed: 12782683]

Wu-Zhang AX, Murphy AN, Bachman M, Newton AC. Isozyme-specific interaction of protein kinase Cdelta with mitochondria dissected using live cell fluorescence imaging. J Biol Chem. 2012; 287:37891–37906. [PubMed: 22988234]

Wynne JP, Wu J, Su W, Mor A, Patsoukis N, Boussiotis VA, Hubbard SR, Philips MR. Rap1-interacting adapter molecule (RIAM) associates with the plasma membrane via a proximity detector. J Cell Biol. 2012; 199:317–330. [PubMed: 23045549]

Xu RX, Pawelczyk T, Xia TH, Brown SC. NMR structure of a protein kinase C-gamma phorbol-binding domain and study of protein-lipid micelle interactions. Biochemistry. 1997; 36:10709–10717. [PubMed: 9271501]

Yang J, Cron P, Thompson V, Good VM, Hess D, Hemmings BA, Barford D. Molecular mechanism for the regulation of protein kinase B/Akt by hydrophobic motif phosphorylation. Mol Cell. 2002; 9:1227–1240. [PubMed: 12086620]

Yang Y, Igumenova TI. The C-terminal v5 domain of protein kinase calpha is intrinsically disordered, with propensity to associate with a membrane mimetic. PloS one. 2013; 8:e65699. [PubMed: 23762412]

Highlights

- Unprimed PKC is in an open conformation with both ligand-binding C1 domains exposed
- Maturation of PKC masks both its C1A and C1B domains to decrease ligand access
- C1 domain masking tunes PKCs affinity for optimal response to second messengers

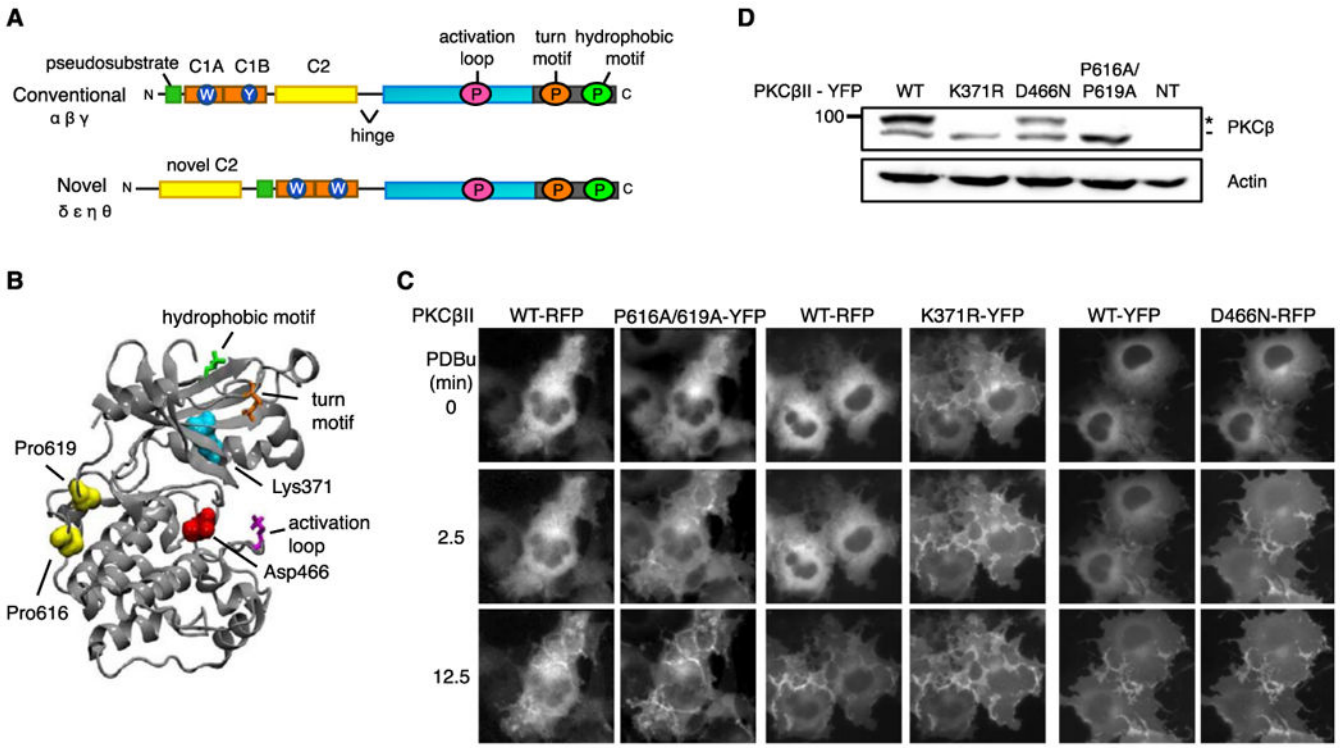

Figure 1.

Maturation of PKC retards agonist-dependent membrane translocation kinetics. (a) Schematic of cPKCs and nPKCs showing domain composition with the C1A and C1B domains (orange) and the C2 domain (yellow). The W and Y are the Trp and Tyr residues at position 22 within the C1A (W58 in PKCβII) or C1B (Y123 in PKCβII) domains of cPKCs that dictate membrane affinity. nPKCs contain Trp at both of these sites. The kinase domain (cyan) and the three priming phosphorylations are shown: the activation loop, turn motif, and hydrophobic motif. (**B**) Ribbon structure of the kinase domain of PKCβII (PDB ID 2I0E) showing the three priming phosphorylations in stick form (Thr500, activation loop; Thr641, turn motif; Ser600, hydrophobic motif) and the kinase-inactivating mutations (Lys371 and AspD466 in the active site and Pro616 and Pro619 in the PXXP motif) in ball form. (**C**) Representative images displaying localization of the indicated YFP- and RFP-tagged PKCs, co-transfected into COS7 cells, before (top), after 2.5 min (middle), or after 12.5 min (bottom) of PDBu treatment are shown. (**D**) Western blot displaying whole-cell lysates of COS7 cells transfected with the indicated PKCβII constructs. The *asterisk* denotes the position of mature, fully phosphorylated PKCβII, and the *dash* denotes the position of unphosphorylated PKCβII.

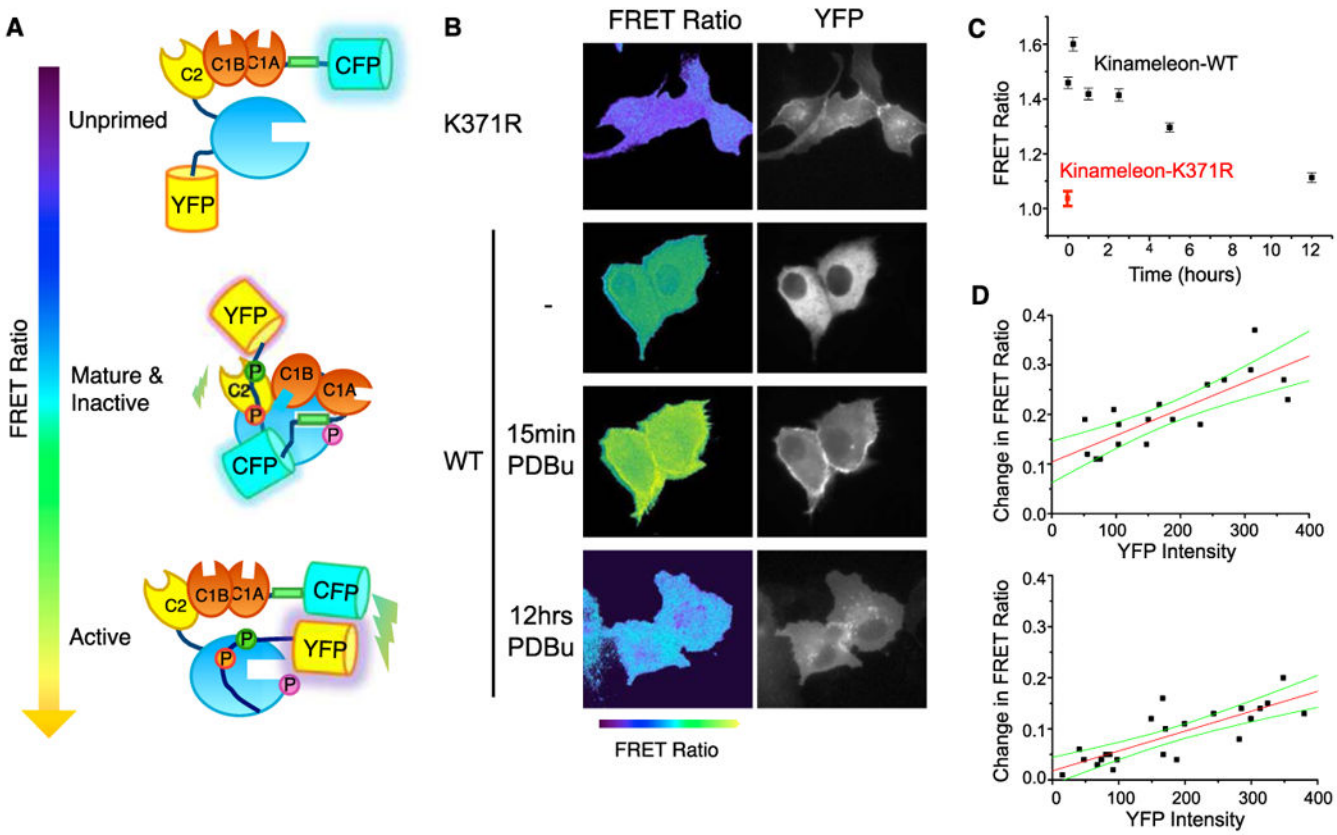

Figure 2.

An intramolecular FRET reporter reads conformational transitions of PKC in live cells. **(A)** Diagram of Kinameleon showing CFP on N-terminus and YFP on C-terminus of PKC; schematic of how very low FRET reflects an unprimed conformation (upper panel), intermediate FRET reflects a mature (phosphorylated at the activation loop in pink, turn motif in orange, and hydrophobic motif in green) but inactive conformation (middle panel), and high FRET reflects an active conformation (lower panel). (**B**) Pseudocolor FRET ratio images (left) and localization (right) of MDCK cells transiently expressing Kinameleon-K371R (representing unprocessed PKC), Kinameleon-WT (representing mature, phosphorylated, but inactive PKC), Kinameleon-WT after 15 min of PDBu treatment (representing mature, active PKC), and Kinameleon-WT after 12 hrs of PDBu treatment (representing dephosphorylated PKC), report different PKC conformations. (**C**) Quantitation of the FRET ratios ± SEM of Kinameleon-WT post PDBu treatment of cells and of Kinameleon-K371R in the absence of PDBu treatment. (**D**) Kinameleon expressed in MDCK cells and stimulated with 200 nM PDBu results in increased FRET, shown as a change in the FRET ratio (upper panel). The increasing FRET change with higher expression levels (linear regression in red, with 95% confidence bands in green) indicates an intermolecular (concentration dependent) interaction. The non-zero y-intercept indicates an intramolecular (concentration-independent) interaction, consistent with a conformational change upon translocation. In contrast, co-expression of CFP-PKCβII-CFP and YFP-PKCβII-YFP show only an intermolecular interaction after 200 nM PDBu (lower panel).

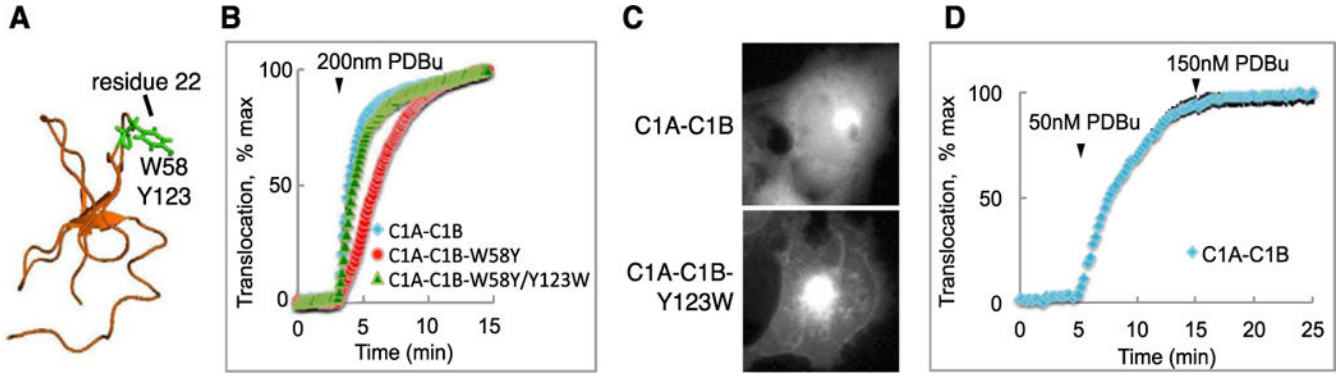

Figure 3.

Translocation kinetics of the isolated C1A-C1B domain of PKCβII can be tuned by a single residue. (**A**) Ribbon structure of the C1B domain of PKCα (PDB ID 2ELI) showing the DAG affinity toggle, Tyr at position 22 in the domain (Tyr123 in PKCα and PKCβ). This residue is present as Trp (Trp58) in the C1A domain of PKCα and PKCβ. (**B**) COS7 cells transfected with the indicated C1A-C1B constructs flanked by CFP and YFP were monitored for their intermolecular FRET ratio ± SEM upon PDBu stimulation. (**C**) Representative YFP images of the basal localization of wild-type or mutant C1A-C1B domains. (**D**) Trace showing translocation kinetics of the C1A-C1B domain ± SEM with sub-saturating levels of phorbol esters (50 nM PDBu), followed by saturating amounts of PDBu to yield a final concentration of 200 nM.

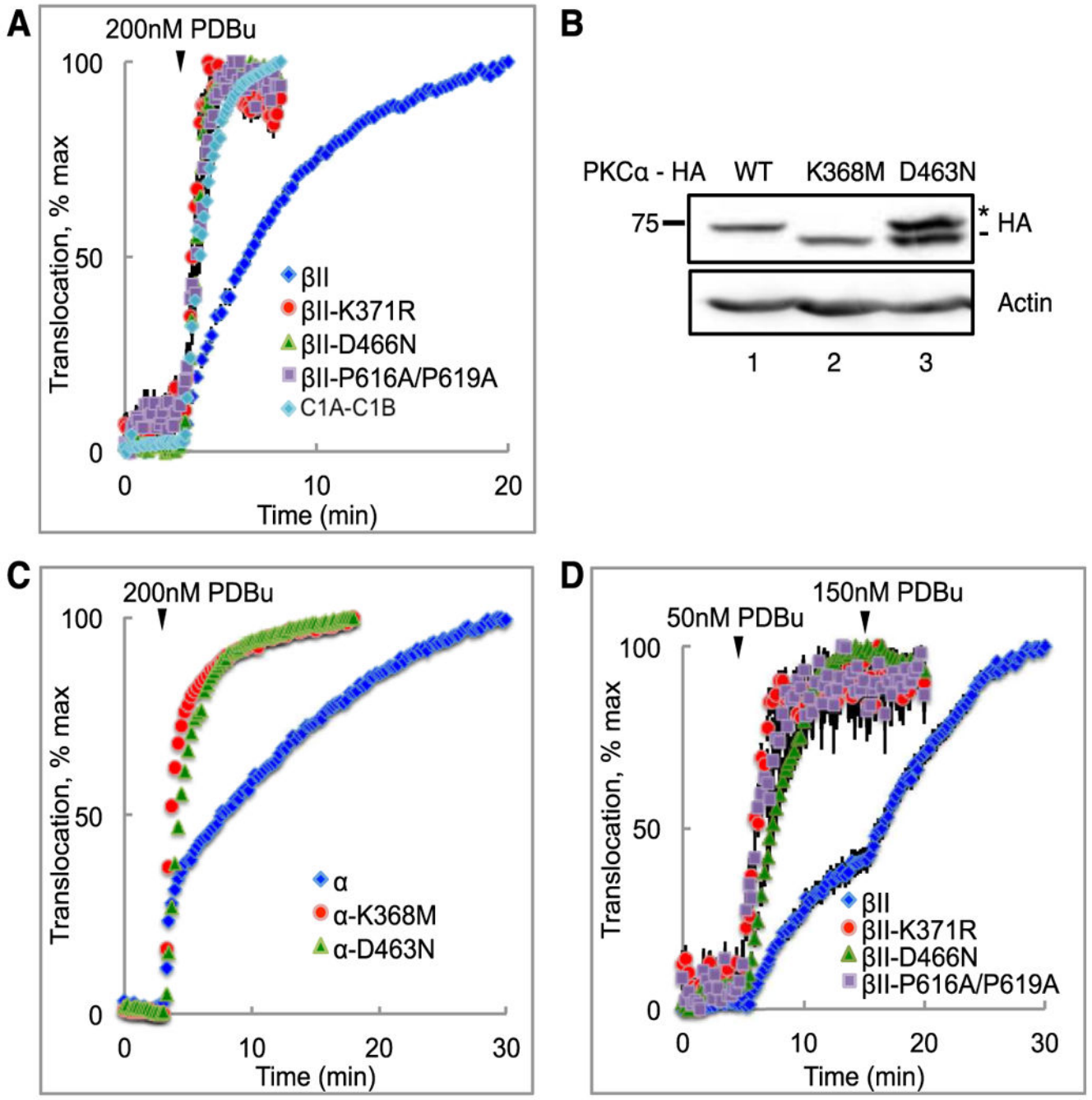

Figure 4.

Unprimed cPKCs have an exposed C1A-C1B tandem module that is masked upon maturation. (**A**) The FRET ratios of COS7 cells co-transfected with membrane-targeted CFP and the indicated full-length, YFP-tagged PKCβII constructs were monitored upon PDBu treatment. Plots show data normalized to 100% for the maximal FRET response ± SEM. (**B**) Western blot of whole-cell lysates of COS7 cells transfected with the indicated HA-PKCα constructs. The *asterisk* denotes the position of mature, fully phosphorylated PKCα, and the *dash* denotes the position of unphosphorylated PKCα. (**C**) FRET ratios ± SEM of COS7

cells co-transfected with membrane-targeted CFP and the indicated full-length, YFP-tagged PKCα constructs were monitored upon PDBu stimulation. (**D**) FRET ratios ± SEM of COS7 cells co-transfected with membrane-targeted CFP and the indicated full-length, YFP-tagged PKCβII constructs were monitored upon stimulation with a sub-saturating PDBu concentration for wild-type PKCβII (50 nM), followed by treatment with another 150 nM PDBu to evoke a maximal response.

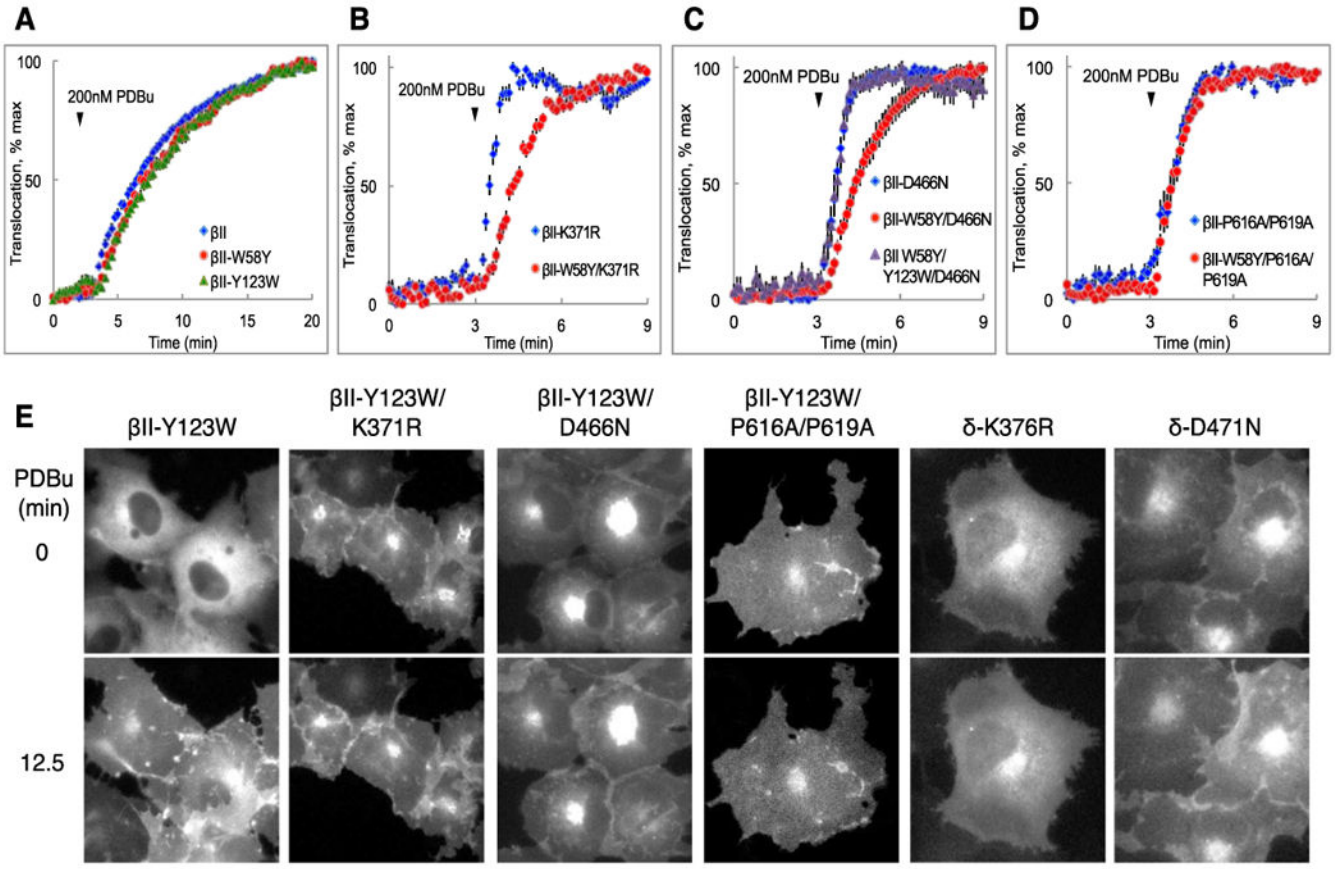

Figure 5.

Both the C1A and C1B domains of unphosphorylated PKCs are exposed and become masked upon priming of PKC. (**A-D**) FRET ratios ± SEM of COS7 cells co-transfected with membrane-targeted CFP and the indicated full-length, YFP-tagged PKCβII constructs were monitored upon PDBu treatment. (**E**) Representative YFP images of localization of the indicated PKCβII or PKCδ mutants before (top) or after (bottom) PDBu treatment.

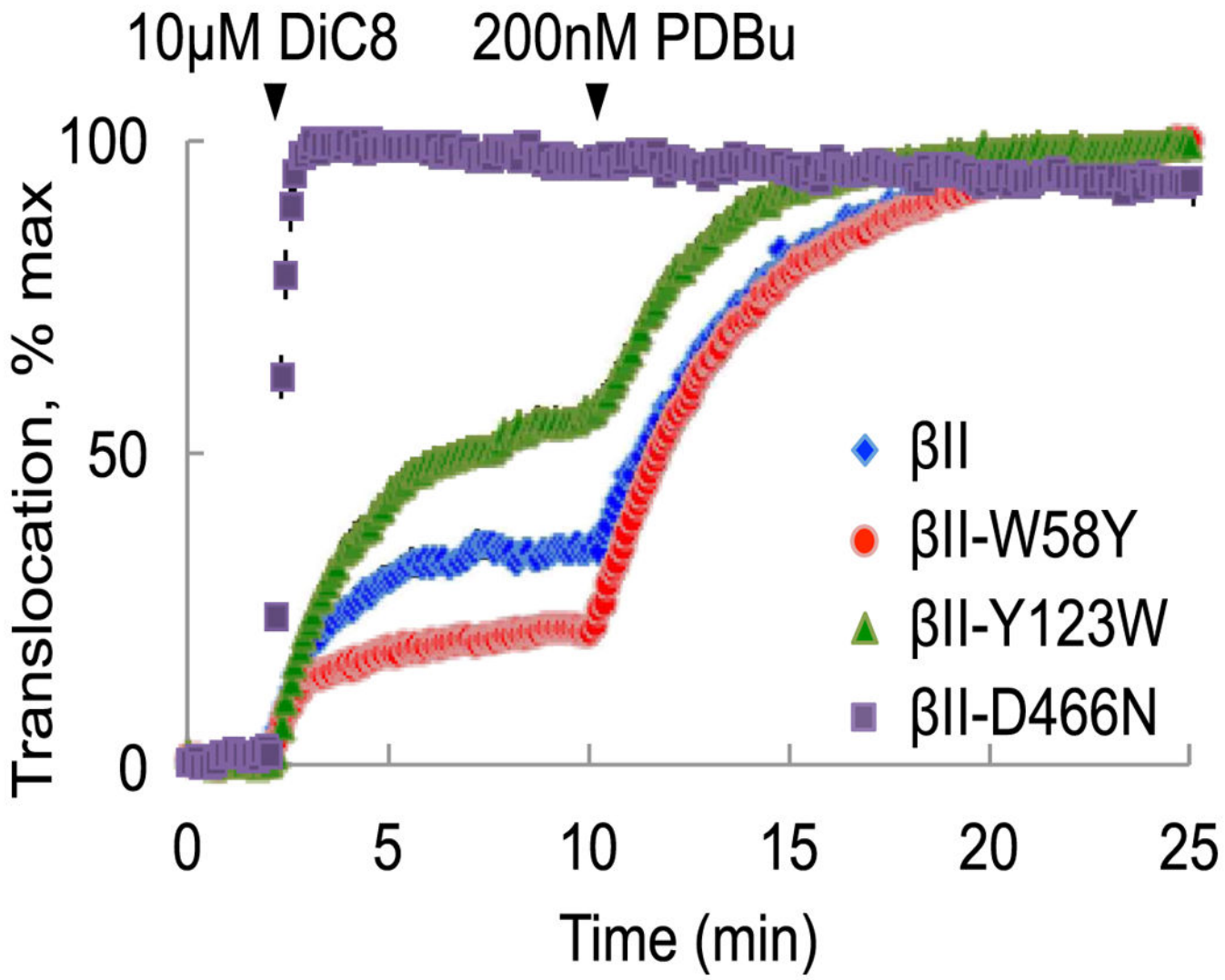

Figure 6.

Both the C1A and C1B domains are involved in membrane binding, but the C1B domain dominates. The FRET ratios ± SEM of COS7 cells co-transfected with membrane-targeted CFP and the indicated full-length, YFP-tagged PKCβII constructs were monitored upon stimulation with the PKC agonists DiC8 and PDBu.

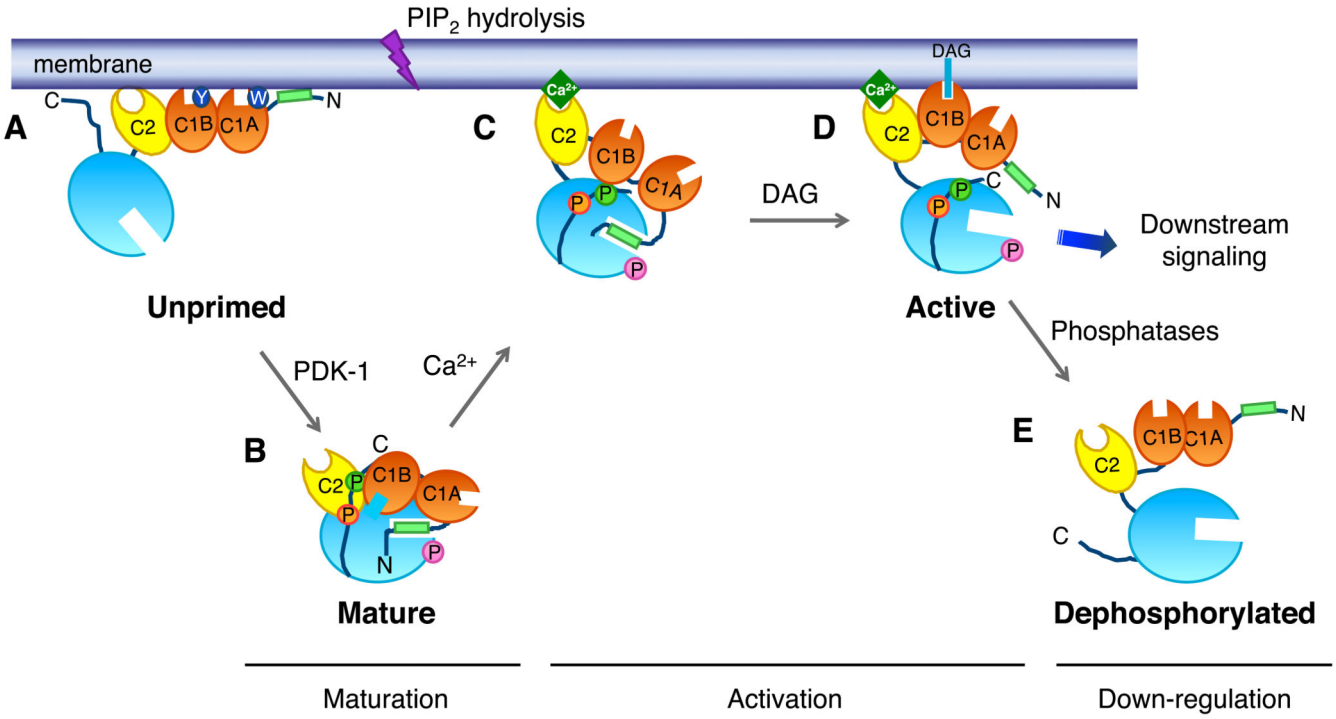

Figure 7.

Model showing how maturation of cPKC masks C1 domains to increase the dynamic range of DAG sensing and thus PKC output. (**A**) Unprimed PKC is in an open conformation that associates with membranes via weak interactions from the C2 domain, both C1A and C1B domains, the exposed pseudosubstrate, and the C-terminal tail. In this conformation, both C1A and C1B domains are fully exposed. (**B**) Upon ordered phosphorylation of PKC at its activation loop (pink), turn motif (orange), and hydrophobic motif (green) sites, PKC matures into its closed conformation, in which both the C1A and C1B domains become masked, the pseudosubstrate binds the substrate binding site, and the enzyme localizes to the cytosol. This masking of the C1 domains prevents pretargeting of PKC to membranes in the absence of agonist-evoked increases in DAG, thus decreasing basal signaling. (**C**) In response to agonists that promote PIP_2 hydrolysis, Ca^{2+}-dependent binding of the C2 domain of cPKCs to the plasma membrane allows the low-affinity DAG sensor to find its membrane-embedded ligand, DAG. (**D**) Binding of DAG, predominantly to the C1B domain of PKCβII, expels the pseudosubstrate from the substrate-binding cavity and activates PKC. Use primarily of the lower-affinity C1B domain increases the dynamic range of PKC output as the signal does not saturate as readily using the lower affinity module and allows cPKCs to signal at the plasma membrane as opposed to the Golgi. (**E**) Dephosphorylation of activated PKC allows it to regain the exposed (open) conformation of unprimed PKC.